

This is an Accepted Manuscript version of the following article, accepted for publication in:

I. Gómez, S. Zarate, G. Almandoz, J. Poza, G. Ugalde and A. J. Escalada, "Analytical model to calculate magnetic flux density in permanent magnet synchronous machines with static eccentricity," 2016 XXII International Conference on Electrical Machines (ICEM), 2016, pp. 152-158.

DOI: <https://doi.org/10.1109/ICELMACH.2016.7732520>

© 2016 IEEE. Personal use of this material is permitted. Permission from IEEE must be obtained for all other uses, in any current or future media, including reprinting/republishing this material for advertising or promotional purposes, creating new collective works, for resale or redistribution to servers or lists, or reuse of any copyrighted component of this work in other works.

# Analytical Model to Calculate Magnetic Flux Density in Permanent Magnet Synchronous Machines with Static Eccentricity

Iratxo Gómez, Sergio Zarate, Gaizka Almandoz, Javier Poza,  
Gaizka Ugalde, Ana Julia Escalada

**Abstract**—In this article a general analytical model for the analysis of permanent magnet synchronous machines with static eccentricity is presented. The model is a continuation of [1] and it is based on Fourier time-space series formulated in 2-D coordinates. The results of the model are corroborated by simulations of finite element method over two different machines. The results of the model show a good agreement with the results obtained from simulations.

**Index Terms**—Finite element method; Fourier time-space series; Permanent-magnet synchronous machine; Static Eccentricity

## I. INTRODUCTION

THE main reason for breakdown in electric machines is the incorrect setting of the machines in the application [2]–[4] and as it is stated in [2] a lot of these faults can be avoided just by oversizing the machines. For instance, it is preferable to oversize the machines thermally which work in hot environments than design them to work near their thermic limit. On the other hand, in [2]–[9] it is illustrated that faults occurred in rotors and bearings, which are inherent to the machines, compute more than fifty percent of all faults in electric machines, see the Fig. 1. In [10]–[13] it is explained that eccentricities appear in the machines due to inevitable mechanical tolerances, in either bearing or couplings, and bending of the rotor, among others. These eccentricities can be classified as static, dynamic and mixed [14]–[17]. The static eccentricity appears when the rotating point of the rotor is the centre of the rotor but it is not aligned with the centre of the stator. It is known as dynamic eccentricity when the rotating point of the rotor is not aligned with its own centre, but it is aligned with the centre of the stator. Finally, mixed eccentricity takes place when the previously described two eccentricities are combined. In this case, the rotating point of the rotor is not aligned with the centre of the rotor nor with the centre of the stator. These eccentricities are shown in the Fig. 2. Regardless of the type of eccentricity, the misalignment between the stator and the rotor generates a non-uniform length of the air-gap [7]. This non-uniform length creates unbalanced flux densities originating unbalanced normal forces which tend to bend the shaft with positive feedback behaviour [10], [11]. That is the reason why, an early detection of eccentricity faults can avoid expensive reparations [4].

In this article an analytical model for the analysis of superficial permanent magnet synchronous machines (PMSMs) with static eccentricity is presented. The model is a continuation of [1] and it is based on Fourier time-space series formulated in 2-D coordinates. Besides, the equations of the model only use design parameters of the machine. Using this model, it can be established the harmonic orders of the magnetic flux densities. Thus, through the checks in the machine, eccentricities can be detected in early stages avoiding expensive reparations in the electrical machines. The presented model has been validated by simulations of finite element method (FEM) over the two machines which are described in Table I.

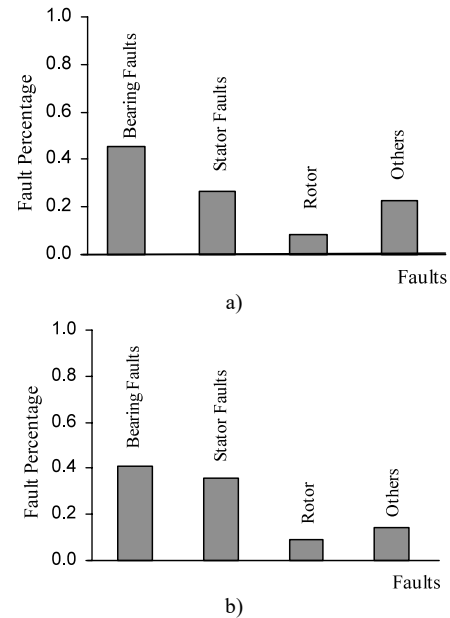


Fig. 1. Location of the faults in electric machines. a) IEEE study and b) EPRI study. [4]

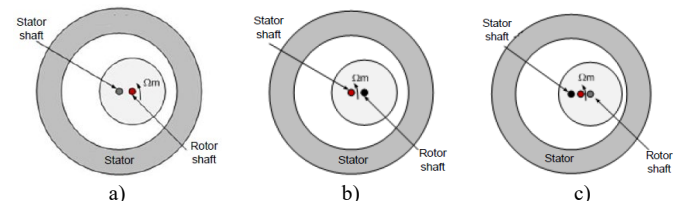


Fig. 2. Types of eccentricity. a) Static; b) Dynamic and c) Mixed. The red shaft represents the rotation axis.

I. Gómez, S. Zarate, G. Almandoz, J. Poza, and G. Ugalde are with the University of Mondragón, 20500 Arrasate – Mondragón.

A.J. Escalada is with ORONA Elevator Innovation Centre, 20120 Hernani. (e-mail: igomez@mondragon.edu; szarate@mondragon.edu; galmandoz@mondragon.edu; jpoza@mondragon.edu; ugalde@mondragon.edu; ajescalada@orona-group.com).

TABLE I  
PRINCIPAL CHARACTERISTICS OF SIMULATED MACHINES.

| Machine | Number of slots | Number of pole pair | Number of winding layers |
|---------|-----------------|---------------------|--------------------------|
| Qs48p8  | 48              | 8                   | 1                        |
| Qs36p15 | 36              | 15                  | 2                        |

## II. ANALYTICAL MODEL

In this section it is explained the proposed analytical model. This model is based on Fourier time-space series and it has been developed in five steps. In the first two steps the computation of flux densities created by magnets and coils in a slotless machine is addressed. In the next two steps, effects due to slots and eccentricity are included in the computation of magnetic flux densities. Finally, both flux densities are superimposed in order to obtain the overall flux density at load conditions with eccentricity. Since this model is based on [1], a previous article, only the necessary mathematical expressions will be stated.

### A. Magnetic Flux Density Created by Magnets in a Slotless Machine

In PMSMs the time-space distribution of the flux density created by magnets can be represented by Fourier series, (1).

$$B_g^m(t, \theta) = \sum_{n=-\infty}^{n=+\infty} \overrightarrow{B_{gn}^m} e^{-jpn(\varphi_m + \Omega_m t - \theta)} \quad (1)$$

Where  $\overrightarrow{B_{gn}^m}$  are the coefficients of the Fourier series,  $p$  is the number of pole pairs,  $n$  is the order of the harmonic,  $\varphi_m$  is the initial position of the magnets and  $\Omega_m$  is the mechanical speed. As it is explained in [1] the coefficients of the Fourier series are computed taking into account the fringing effect. Including this effect more realistic spatial distribution of the flux density is obtained and in this way the accuracy of the results is increased. In this article, the fringing coefficient is parameterized as a function of different dimensions of the machine so as to find a physical meaning, [18]–[20].

### B. Magnetic Flux Density Created by Coils in a Slotless Machine

Magnetic flux density created by coils in the air-gap is calculated by (2).

$$B_g^a(t, \theta) = \mu_0 \cdot \frac{F_{MM}(t, \theta)}{g + \frac{h_m}{\mu_{rm}}} \quad (2)$$

$g$  represents the length of the air-gap,  $\mu_0$  the permeance of the air,  $\mu_{rm}$  the relative permeability of the magnets,  $h_m$  the height of the magnets and  $F_{MM}$  the magnetomotive force created by the coils in the air-gap. The distribution of the stator coils must be known to calculate the  $F_{MM}$ . This distribution is defined as the variation of the magnetomotive force per unit of current in the air-gap and it can be obtained applying the well-known star of slots method. Once the physical distribution of the conductors is known, Fig. 3, the magnetomotive force per current unit can be computed by (3).

$$F_a(\theta) = \sum_{n=-\infty}^{n=+\infty} \overrightarrow{F_{an}} e^{-jnt_p\theta} \quad (3)$$

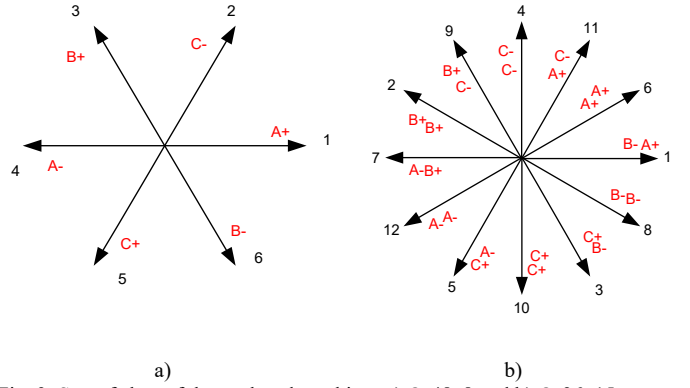


Fig. 3. Star of slots of the analysed machines a) Qs48p8 and b) Qs36p15.

Where  $\overrightarrow{F_{an}}$  are coefficients of the Fourier series and  $t_p$  is the periodicity of the stator winding, which is defined as the greatest common divisor between the number of slots,  $Q_s$ , and  $p$ . Then the magnetomotive force per current of each phase is multiplied by the current of its phase (4) and finally the magnetomotive force of all phases is summed (5).

$$F_{MMa}(t, \theta) = F_a(\theta) \cdot i_A(t) \quad (4)$$

$$F_{MM}(t, \theta) = F_{MMa}(t, \theta) + F_{MMb}(t, \theta) + F_{MMc}(t, \theta) \quad (5)$$

Finally (2) is applied in order to compute the flux density produced by coils. It is important to note that the phase difference between magnetomotive forces of different phases is the same as between currents,  $2\pi/3$  radians. That is the reason why (6) can be obtained from (5).

$$F_{MM}(t, \theta) = \sum_{n=-\infty}^{n=+\infty} \overrightarrow{F_{an}} d_n e^{-jnt_p\theta} i e^{jW_e t} \quad (6)$$

$$d_n = \left[ 1 + 2 \cos\left(\frac{2\pi}{3}(n-1)\right) \right]$$

Analyzing (6) it can be deduced that in a three-phase machine the overall  $F_{MM}$  does not have harmonics multiples of 3.

### C. Effects of Slots and Static Eccentricity

As it is stated in [1] to include the variation of the permeance due to the slots in the model, first of all, the permeance of a slot must be computed. This effect is obtained in [18], [21] through a conformal transformation from Z to W plane, but this calculus was firstly introduced by Zhu in [22].

When the variation of the permeance of a slot is obtained, the variation for whole machine can be reconstructed with (7).

$$(\theta) = \lambda_0 + \sum_{n=1}^{+\infty} \overrightarrow{\lambda_n} \cos(Q_s n(\theta_s - \theta)) \quad (7)$$

Where  $\lambda_0$  is the mean value of the variation of the permeance,  $\lambda_n$  are the coefficients of the Fourier series and  $\theta_s$  is the initial angle position of the slot. When it is needed to analyse the machine without the slots effect,  $\lambda_0 = 1$  and  $\lambda_n = 0$

must be set. On the other hand, to represent the flux density in slotted machines, (1) and (7) must be multiplied.

To include the static eccentricity in the model firstly, the effect of the static eccentricity must be defined, (8).

$$\Delta_\epsilon(\theta) = 1 + \sum_{v=-1}^{v=1} \Delta e^{-jv\theta} \quad (8)$$

Where  $\Delta$  is the variation of the length of the air-gap due to the eccentricity and it can be calculated by (9).

$$\Delta = \frac{\epsilon}{g + \frac{h_m}{\mu_{rm}}} \quad (9)$$

$\epsilon$  is the distance between the axis of the stator and the rotor, Fig. 4. Once the eccentricity is modelled, the magnetic flux densities must be multiplied by it, see (10) for the magnetic flux density created by magnets and (11) for the magnetic flux density created by stator coils. In this case, the machine also can be analysed with and without eccentricity. To remove the effect of the eccentricity, the next parameter must be set:  $\epsilon = 0$ , so  $\Delta_\epsilon(\theta) = 1$ . This define the length of the air-gap as a constant which does not depend on the position of the rotor.

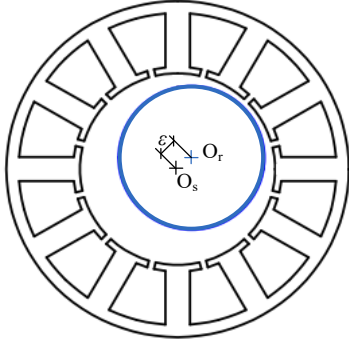


Fig. 4. Distance between the axis of the stator and the rotor [14].

$$B_{g\epsilon}^m(t, \theta) = B_g^m(t, \theta) \cdot \Delta_\epsilon(\theta) = \sum_{n=-\infty}^{n=+\infty} \vec{B}_{gn}^m e^{-jpn(\varphi_m + \Omega_m t - \theta)} + \sum_{n=-\infty}^{n=+\infty} \sum_{v=-1}^{v=1} \Delta \vec{B}_{gn}^m e^{-jpn(\varphi_m + \Omega_m t)} e^{-jv\theta(n + \frac{v}{p})} \quad (10)$$

$$B_{g\epsilon}^b(t, \theta) = B_g^b(t, \theta) \cdot \Delta_\epsilon(\theta) = \sum_{n=-\infty}^{n=+\infty} \frac{\mu_0 \cdot \vec{F}_{an} \cdot d_n}{g + \frac{h_m}{\mu_{rm}}} e^{-jnp\theta} e^{jW_e t} + \sum_{n=-\infty}^{n=+\infty} \sum_{v=-1}^{v=1} \Delta \frac{\mu_0 \cdot \vec{F}_{an} \cdot d_n}{g + \frac{h_m}{\mu_{rm}}} e^{-jnp\theta(n + \frac{v}{p})} e^{jW_e t} \quad (11)$$

From (10) and (11) it can be deduced the Table II and the Table III. The Table II represents the relationship between the harmonics of the flux density created by the magnets in a machine with and without a static eccentricity. On the other

hand, in the Table III the relationship between harmonics of the flux density created by stator coils in a machine with and without static eccentricity are represented. From the Table II and the Table III can be deduced that the unique way to modify the order of the harmonics generated by the static eccentricity is changing the number of pole pairs of the machines.

TABLE II

RELATIONSHIP BETWEEN HARMONICS OF THE FLUX DENSITY CREATED BY MAGNETS IN A MACHINE WITH AND WITHOUT STATIC ECCENTRICITY. A) TEMPORAL DISTRIBUTION AND B) SPATIAL DISTRIBUTION

| A)  |  |
|---|--|
| HARMONICS OF THE MAGNETIC FLUX DENSITY WITHOUT ECCENTRICITY | HARMONICS OF THE MAGNETIC FLUX DENSITY WITH ECCENTRICITY |
| $n$   | $\epsilon_m = \pm n$                                     |
| $\pm 1$   | $\pm 1$  |
| $\pm 3$   | $\pm 3$  |
| $\pm 5$   | $\pm 5$  |
| $\pm 7$   | $\pm 7$  |
| $\pm 9$   | $\pm 9$  |

| B)  |                                      |  |
|---|--------------------------------------|--|
| Harmonics of the magnetic flux density without eccentricity | Harmonics of the static eccentricity | Harmonics of the magnetic flux density due to eccentricity |
| $n$   | $v/p$                                | $\epsilon_m = \pm n \pm v/p$                               |
| $\pm 1$   | $\pm 1/p$                            | $\pm 1 \pm 1/p$  |
| $\pm 3$   | $\pm 1/p$                            | $\pm 3 \pm 1/p$  |
| $\pm 5$   | $\pm 1/p$                            | $\pm 5 \pm 1/p$  |
| $\pm 7$   | $\pm 1/p$                            | $\pm 7 \pm 1/p$  |
| $\pm 9$   | $\pm 1/p$                            | $\pm 9 \pm 1/p$  |

TABLE III

RELATIONSHIP BETWEEN HARMONICS OF THE FLUX DENSITY CREATED BY STATOR COILS IN A MACHINE WITH AND WITHOUT STATIC ECCENTRICITY. A) TEMPORAL DISTRIBUTION AND B) SPATIAL DISTRIBUTION

| A)  |  |
|---|--|
| HARMONICS OF THE MAGNETIC FLUX DENSITY WITHOUT ECCENTRICITY | HARMONICS OF THE MAGNETIC FLUX DENSITY WITH ECCENTRICITY |
| $k$   | $\epsilon_m = \pm n$                                     |
| $\pm 1$   | $\pm 1$  |
| $\pm 5$   | $\pm 5$  |
| $\pm 7$   | $\pm 7$  |
| $\pm 11$  | $\pm 11$   |
| $\pm 13$  | $\pm 13$   |

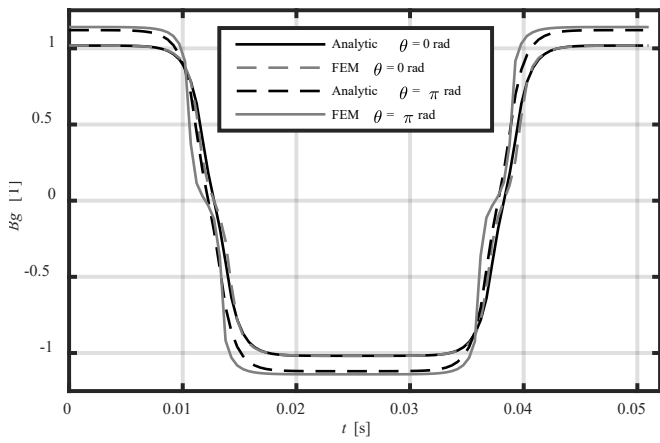
  

| B)  |                                      |  |
|---|--------------------------------------|--|
| Harmonics of the magnetic flux density without eccentricity | Harmonics of the static eccentricity | Harmonics of the magnetic flux density due to eccentricity |
| $n \cdot tp/p$  | $v/p$                                | $\epsilon_m = \pm n \cdot tp/p \pm v/p$                    |
| $\pm 1 \cdot tp/p$  | $\pm 1/p$                            | $\pm 1 \cdot tp/p \pm 1/p$                                 |
| $\pm 5 \cdot tp/p$  | $\pm 1/p$                            | $\pm 5 \cdot tp/p \pm 1/p$                                 |
| $\pm 7 \cdot tp/p$  | $\pm 1/p$                            | $\pm 7 \cdot tp/p \pm 1/p$                                 |
| $\pm 11 \cdot tp/p$   | $\pm 1/p$                            | $\pm 11 \cdot tp/p \pm 1/p$                                |
| $\pm 13 \cdot tp/p$   | $\pm 1/p$                            | $\pm 13 \cdot tp/p \pm 1/p$                                |

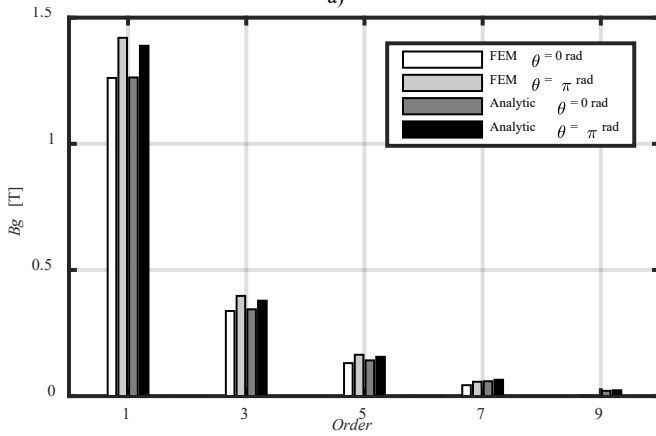
### III. VALIDATION

The results of the developed analytical model are corroborated by FEM software, specifically by Flux-CEDRAT®. The comparison has been realized with the two machines of the Table I. One of these machines is an integer machine (Qs48p8) and the other one is a fractional machine (Qs36p15). The grade of the static eccentricity,  $e$ , in both machines is 30% which has been calculated by (12).

$$\epsilon = g \cdot e \quad (12)$$

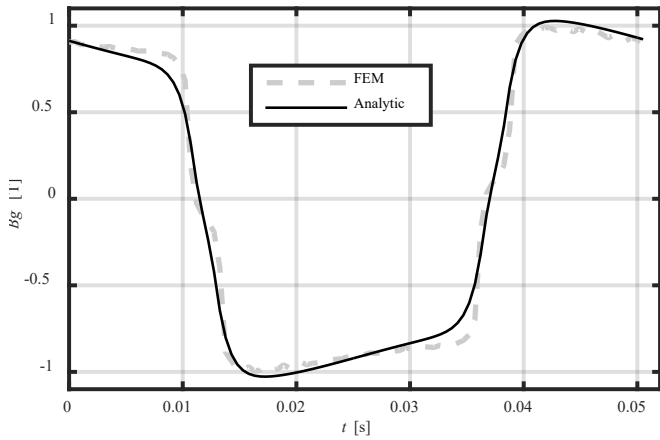


a)

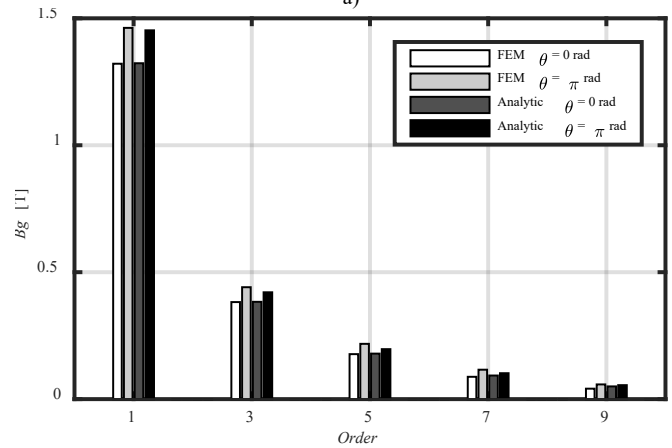


b)

Fig. 5. Temporal distributions of the magnetic flux density in the air-gap of the Qs48p8 at open circuit condition with a 30% of static eccentricity. a) Temporal waves and b) Spectrums.

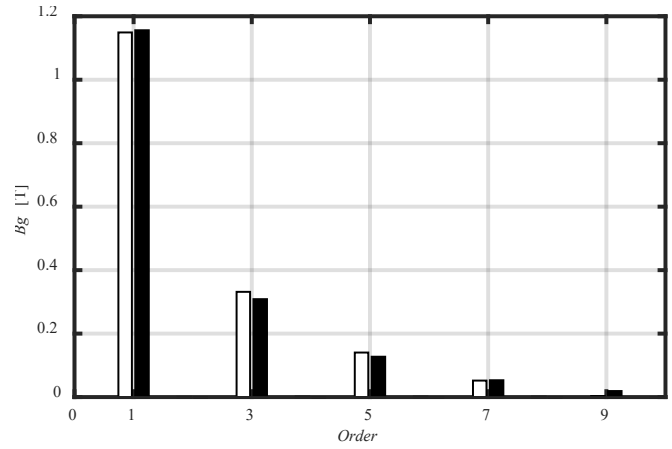


a)



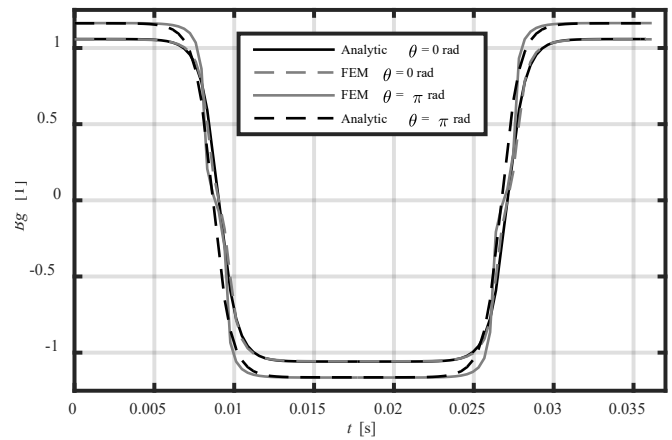
b)

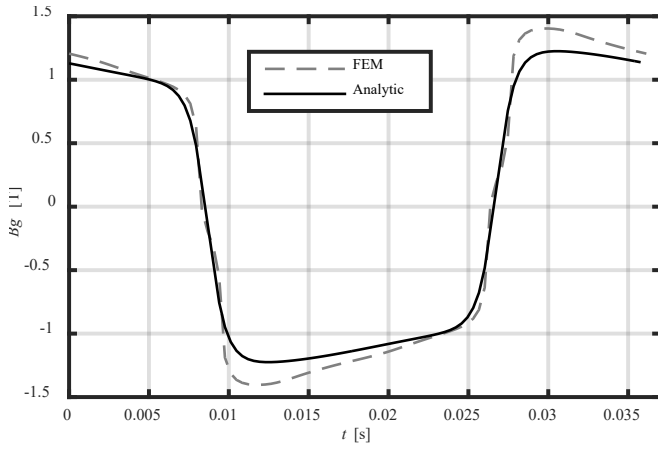
Fig. 7. Temporal distributions of the magnetic flux density in the air-gap of the Qs36p15 at open circuit condition with a 30% of static eccentricity. a) Temporal waves and b) Spectrums.



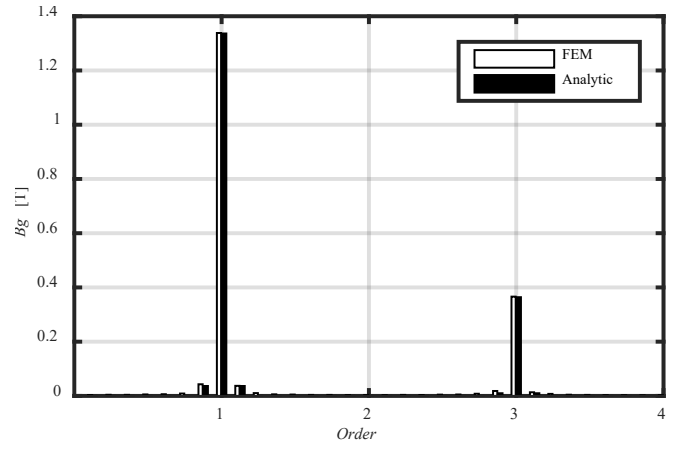
b)

Fig. 6. Temporal distributions of the magnetic flux density in the air-gap of the Qs48p8 at load condition with a 30% of static eccentricity. a) Temporal waves and b) Spectrums.

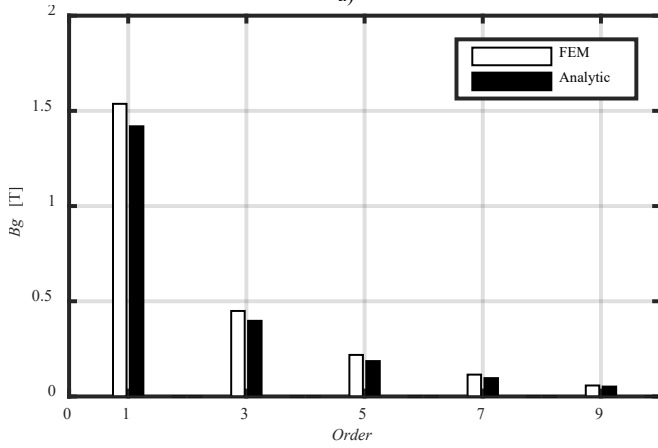




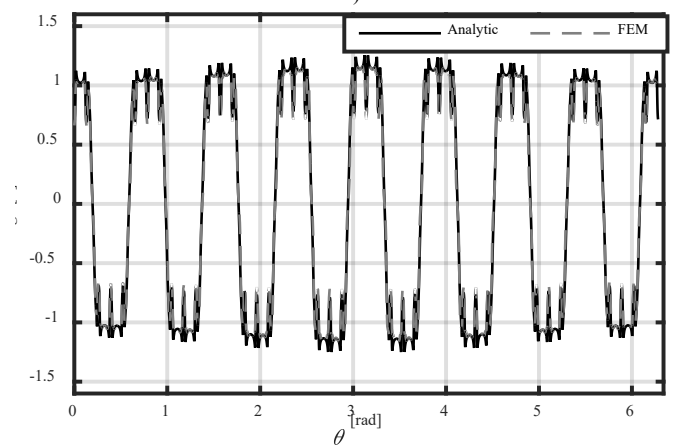
a)



b)



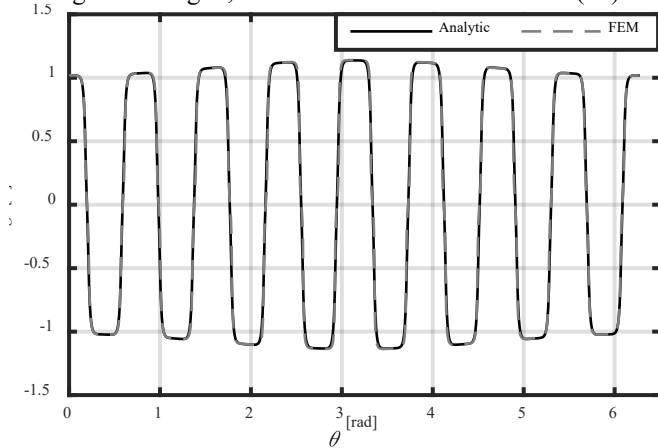
b)



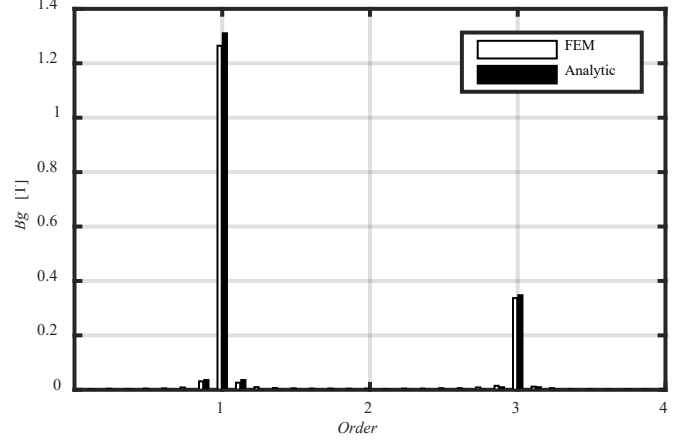
c)

Fig. 8. Temporal distributions of the magnetic flux density in the air-gap of the Qs36p15 at load condition with a 30% of static eccentricity. a) Temporal waves and b) Spectrums.

From the Fig. 5 to the Fig. 8 the waves and spectrums of the temporal distributions of the magnetic flux density in the air-gap are shown. As it has been explained in section II.C and it can be corroborated in these figures, the static eccentricity does not create new harmonics in the temporal distribution. In addition, all harmonics are integer and odd, despite of the topology of the machine, integer or fractional. However, it can be seen that depending on the position in which the path is collocated, the amplitude of the wave and harmonics change, see Fig. 5 and Fig. 7, such as it can be deduced from (10)

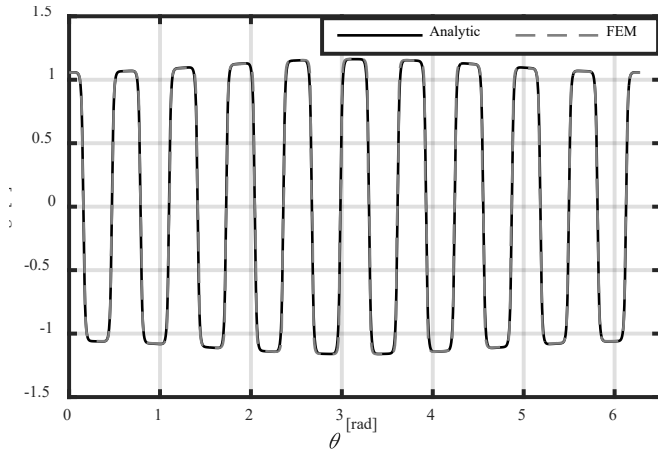


a)

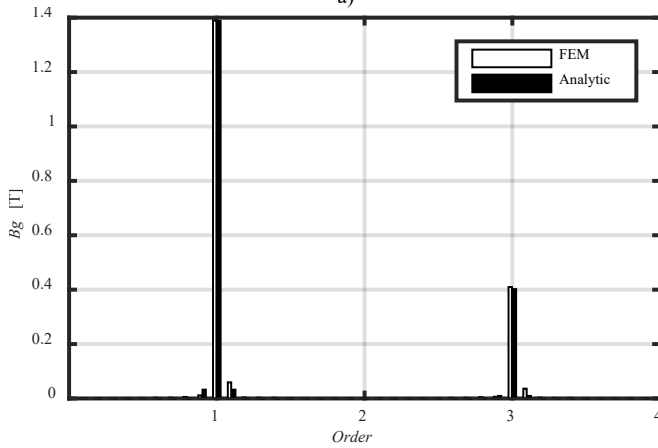


d)

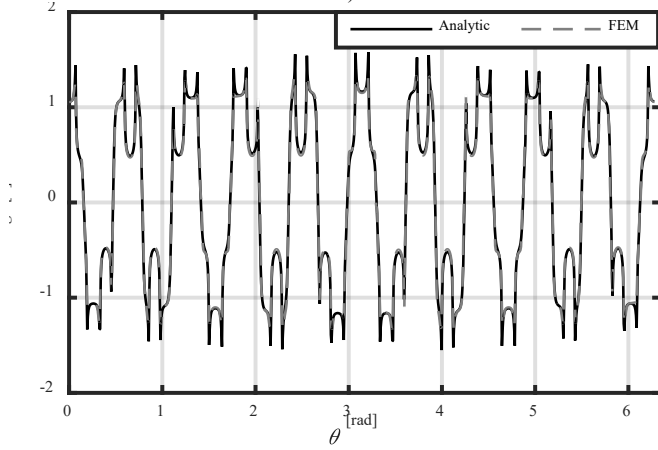
Fig. 9. Spatial distributions of the magnetic flux density in the air-gap of the Qs48p8 machine at open circuit condition with a 30% of static eccentricity .a) Spatial waves in a slotless machine b) Spectrums in a slotless machine; c) Spatial waves in a slotted machine and d) Spectrums in a slotted machine.



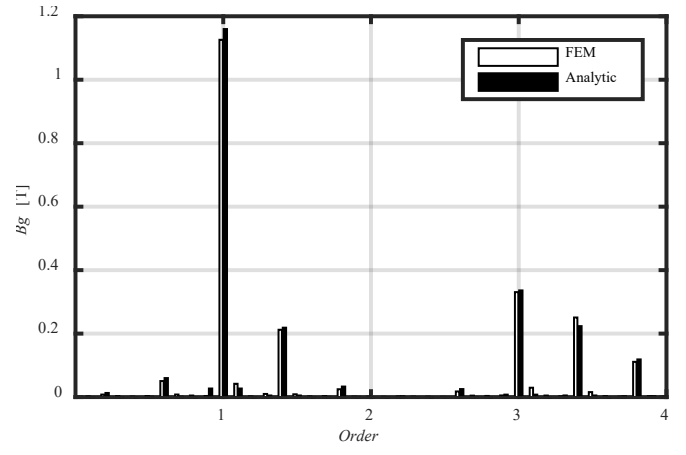
a)



b)



c)



d)

Fig. 10. Spatial distributions of the magnetic flux density in the air-gap of the Qs36p15 machine at open circuit condition with a 30% of static eccentricity a) Spatial waves in a slotless machine b) Spectrums in a slotless machine; c) Spatial waves in a slotted machine and d) Spectrums in a slotted machine.

In the Fig. 9 and the Fig. 10 the waves and spectrums of the spatial distributions of the magnetic flux density in the air-gap are illustrated. In this case, in the Fig. 9-b and the Fig. 10-b it can be corroborated that static eccentricity creates new harmonics. As it has been explained in section II.C these new harmonics appear in both sides of the principal harmonic. That is the reason why there are not only odd and integer harmonics. However, in the Fig. 9-d and the Fig. 10-d there are more harmonics. These harmonics are created by the slots of the machine and that is why they are related to the number of slots of the machine.

#### IV. CONCLUSIONS

This article presents an analytical model for the analysis of PMSMs with static eccentricity. The model is based on Fourier time-space series formulated in 2-D coordinates. This model can be used to represent the magnetic flux density created in a machine at open circuit and load operation conditions with and without slots and static eccentricity.

Two machines are studied by FEM software, concretely with Flux-CEDRAT<sup>®</sup>, to corroborate the results of the analytical model. The types of machines that have been considered are: a fractional machine with 36 slots in the stator and 30 poles in the rotor, and an integer machine with 48 slots in the stator and 16 poles in the rotor. The obtained results for magnetic flux densities demonstrated that magnitudes and frequencies of main harmonics are computed with rather good accuracy. So, it can be affirmed that the model shows a good agreement with the FEM results especially in the identification of the harmonics.

The main advantages of the model compared to the FEM simulations are the rapidity of the calculations and the easiness to relate components of the flux density to design variables. That is why, using the proposed model, an identification of the harmonics of the magnetic flux density in the air-gap with static eccentricity can be done easily and in a quickly way.

Further work will be needed to include into the model the dynamic eccentricity effect. A part from that, a prototype will be built in order to validate the model experimentally.

## V. REFERENCES

- [1] I. Gomez, G. Almandoz, J. Poza, G. Ugalde, and A. J. Escalada, "Analytical Model to Calculate Radial Forces in Permanent-Magnet Synchronous Machines," *Electrical Machines (ICEM), 2014 International Conference on*, pp. 2681–2687, 2014.
- [2] P. Tavner, L. Ran, J. Penman, and H. Sedding, "Review of Condition Monitoring of Rotating Electrical Machines," *IET*, vol. 56, pp. 1–277, 2008.
- [3] M. E. H. Benbouzid, "A Review of Induction Motors Signature Analysis as a Medium for Faults Detection," *IEEE Trans. Ind. Electron.*, vol. 47, no. 5, pp. 984–993, 2000.
- [4] G. K. Singh and S. Ahmed Saleh Al Kazzaz, "Induction machine drive condition monitoring and diagnostic research—a survey," *Electr. Power Syst. Res.*, vol. 64, no. 2, pp. 145–158, Feb. 2003.
- [5] R. R. Moghaddam, "Synchronous Reluctance Machine (SynRM) in Variable Speed Drives (VSD) Applications," KTH, 2011.
- [6] C. Verucchi and G. Acosta, "Técnicas de Detección y Diagnóstico de fallos en Máquinas Eléctricas de Inducción," *IEEE Lat. Am. Trans.*, vol. 5, no. 1, pp. 41–49, 2007.
- [7] Y. Da, X. Shi, and M. Krishnamurthy, "Health Monitoring, Fault Diagnosis and Failure Prognosis Techniques for Brushless Permanent Magnet Machines," *2011 Veh. Power Propuls. Conf. VPPC*, pp. 1–7, 2011.
- [8] A. H. Bonnet and G. C. Soukup, "Analysis of Rotor Failures in Squirrel-Cage Induction Motors," *IEEE Trans. Ind. Appl.*, vol. 24, no. 6, pp. 1124–1130, 1988.
- [9] G. Stone, E. A. Boulter, I. Culbert, and H. Dhirani, *Electrical insulation for rotating machines: design, evaluation, aging, testing, and repair*, vol. 21. John Wiley & Sons, 2004.
- [10] L. Cappelli, Y. Coia, F. Marignetti, and Z. Q. Zhu, "Analysis of Eccentricity in Permanent-Magnet Tubular Machines," *Industrial Electronics, IEEE Transactions on*, vol. 61, no. 5, pp. 2208–2216, 2014.
- [11] J. a. Rosero, J. Cusido, a. Garcia, J. a. Ortega, and L. Romeral, "Study on the Permanent Magnet Demagnetization Fault in Permanent Magnet Synchronous Machines," *IECON 2006 - 32nd Annu. Conf. IEEE Ind. Electron.*, pp. 879–884, Nov. 2006.
- [12] W. le Roux, R. G. Harley, and T. G. Habetler, "Detecting Rotor Faults in Low Power Permanent Magnet Synchronous Machines," *IEEE Trans. Power Electron.*, vol. 22, no. 1, pp. 322–328, Jan. 2007.
- [13] W. Row, R. G. Harley, and T. G. Habetler, "Detecting Rotor Faults in Permanent Magnet Synchronous Machines," *2003 Symp. Diagnostics Electr. Mach. Power Electron. Drives, SDEMPED*, pp. 24–26, 2003.
- [14] Z. Q. Zhu, L. J. Wu, and M. L. M. Jamil, "Influence of Pole and Slot Number Combinations on Cogging Torque in Permanent Magnet Machines with Static and Rotating Eccentricities," *Energy Conversion Congress and Exposition (ECCE), 2013 IEEE*, pp. 2834–2841, 2013.
- [15] D.-H. Hwang, J.-H. Chang, D.-S. Kang, J.-H. Lee, and K.-H. Choi, "A Method for Dynamic Simulation and Detection of Air-gap Eccentricity in Induction Motors by Measuring Flux Density," *Electromagnetic Field Computation, 2006 12th Biennial IEEE Conference on*, p. 69, 2006.
- [16] D.-H. Hwang, K.-C. Lee, Y.-J. Kim, Y.-J. Lee, K.-H. Choi, and J.-H. Lee, "A Study on Dynamic Simulation and Detection of Air-Gap Eccentricity in Induction Machines," *Industrial Electronics, 2005. ISIE 2005. Proceedings of the IEEE International Symposium on*, vol. 2, pp. 867–870 vol. 2, 2005.
- [17] H. Qian, H. Guo, Z. Wu, and X. Ding, "Analytical Solution for Cogging Torque in Surface-Mounted Permanent-Magnet Motors With Magnet Imperfections and Rotor Eccentricity," *Magnetics, IEEE Transactions on*, vol. 50, no. 8, pp. 1–15, 2014.
- [18] A. Egea, G. Almandoz, J. Poza, and A. Gonzalez, "Analytic model of axial flux permanent magnet machines considering spatial harmonics," *Power Electron. Electr. Drives Autom. Motion (SPEEDAM), 2010 Int. Symp.*, pp. 495–500, 2010.
- [19] J. R. Hendershot and T. J. E. Miller, *Design of Brushless Permanent-Magnet Machines*. Motor Desing Books, 2010.
- [20] T. J. E. Miller and R. Rabinovici, "Back-EMF Waveforms and Core Losses in Brushless DC Motors," *IEEE Proc. Electr. Power Appl. Proc. Electr. Power Appl.*, vol. 141, no. 3, pp. 144–154, 1994.
- [21] G. Almandoz, J. Poza, M. A. Rodriguez, and A. Gonzalez, "Analytic model of a PMSM considering spatial harmonics," *Power Electron. Electr. Drives, Autom. Motion, 2008. SPEEDAM 2008. Int. Symp.*, pp. 603–608, 2008.
- [22] Z. Q. Zhu and D. Howe, "Instantaneous Magnetic Field Distribution in Brushless Permanent Magnet DC Motors. III. Effect of Stator Slotting," *IEEE Trans. Magn.*, vol. 29, no. 1, pp. 143–151, 1993.

## VI. BIOGRAPHIES

**Iratxo Gómez** was born in Vitoria, Spain, in June 1989. He received the B.S. degree in electrical engineering at the University of Mondragón, Mondragón, Spain, in 2013, where he is currently working toward the Ph.D. degree. His current research interests include electrical machines vibration and noise and permanent magnet machine design and optimization.

**Sergio Zárate** was born in Vitoria, Spain, in September 1990. He received the B.S. degree in electrical engineering at the University of Mondragón, Mondragón, Spain, in 2014, where he is currently working toward the Ph.D. degree. His current research interests include drives, electrical machines vibration and permanent magnet machine design.

**Gaizka Almandoz** was born in Arantz, Spain, in March 1979. He received the B.S. and Ph.D. degrees in electrical engineering at the University of Mondragón, Mondragón, Spain, in 2003 and 2008, respectively. Since 2003, he has been with the Department of Electronics, Faculty of Engineering, University of Mondragón, where he is currently an Associate Professor. His current research interests include electrical machine design, modelling, and control. He has participated in various research projects in the fields of wind energy systems, lift drives, and railway traction.

**Javier Poza** was born in Bergara, Spain, in June 1975. He received the B.S. degree in electrical engineering at the University of Mondragón, Mondragón, Spain, in 1999 and the Ph.D. degree in electrical engineering from the Institut National Polytechnique de Grenoble, Grenoble, France. Since 2002, he has been with the Department of Electronics, Faculty of Engineering, University of Mondragón, where he is currently an Associate Professor. His current research interests include electrical machine design, modelling, and control. He has participated in various research projects in the fields of wind energy systems, lift drives, and railway traction.

**Gaizka Ugalde** was born in Ermua, Spain. He received the B.S. and the Ph.D. degrees in electrical engineering at the University of Mondragón, Mondragón, Spain, in 2006 and 2009, respectively. Since 2009, he has been with the Department of Electronics, Faculty of Engineering, University of Mondragón, where he is currently an Associate Professor. His current research interests include permanent-magnet machine design, modelling, and control. He has participated in various research projects in the fields of lift drives and railway traction.

**Ana Julia Escalada** was born in Pamplona, Spain, in April 1977. She received the B.S. degree in electronic engineering at the University of the Basque Country, Bilbao, Spain, in 2001, the B.S. degree in physics from the University of Cantabria, Santander, Spain, in 2003, and the Ph.D. degree in automatic and industrial electronic engineering at the University of Mondragón, Mondragón, Spain, in 2007, in conjunction with the Power Electronics Department, Ikerlan Technological Research Center.

She is currently with the Electrical Drives Department, ORONA Elevator Innovation Centre, Hernani, Spain. Her interests are drives and electrical machines for lifts.